PROCEEDINGS OF SPIE

SPIEDigitalLibrary.org/conference-proceedings-of-spie

Performance of the Apache Point Observatory Galactic Evolution Experiment (APOGEE) high-resolution near-infrared multi-object fiber spectrograph

Wilson, John, Hearty, F., Skrutskie, M., Majewski, S., Schiavon, R., et al.

John C. Wilson, F. Hearty, M. F. Skrutskie, S. R. Majewski, R. Schiavon, D. Eisenstein, J. Gunn, J. Holtzman, D. Nidever, B. Gillespie, D. Weinberg, B. Blank, C. Henderson, S. Smee, R. Barkhouser, A. Harding, S. Hope, G. Fitzgerald, T. Stolberg, J. Arns, M. Nelson, S. Brunner, A. Burton, E. Walker, C. Lam, P. Maseman, J. Barr, F. Leger, L. Carey, N. MacDonald, G. Ebelke, S. Beland, T. Horne, E. Young, G. Rieke, M. Rieke, T. O'Brien, J. Crane, M. Carr, C. Harrison, R. Stoll, M. Vernieri, M. Shetrone, C. Allende-Prieto, J. Johnson, P. Frinchaboy, G. Zasowski, A. Garcia Perez, D. Bizyaev, K. Cunha, V. V. Smith, Sz. Meszaros, B. Zhao, M. Hayden, S. D. Chojnowski, B. Andrews, C. Loomis, R. Owen, M. Klaene, J. Brinkmann, F. Stauffer, D. Long, W. Jordan, D. Holder, F. Cope, T. Naugle, B. Pfaffenberger, D. Schlegel, M. Blanton, D. Muna, B. Weaver, S. Snedden, K. Pan, H. Brewington, E. Malanushenko, V. Malanushenko, A. Simmons, D. Oravetz, S. Mahadevan, S. Halverson, "Performance of the Apache Point Observatory Galactic Evolution Experiment (APOGEE) high-resolution near-infrared multi-object fiber spectrograph," Proc. SPIE 8446, Ground-based and Airborne Instrumentation for Astronomy IV, 84460H (24 September 2012); doi: 10.1117/12.927140

SPIE.

Event: SPIE Astronomical Telescopes + Instrumentation, 2012, Amsterdam, Netherlands

Downloaded From: https://www.spiedigitallibrary.org/conference-proceedings-of-spie on 06 Jan 2021 Terms of Use: https://www.spiedigitallibrary.org/terms-of-use

Performance of the Apache Point Observatory Galactic Evolution Experiment (APOGEE) high-resolution near-infrared multi-object fiber spectrograph

John C. Wilson*[a], F. Hearty[a], M. F. Skrutskie[a], S. R. Majewski[a], R. Schiavon[b], D. Eisenstein[c], J. Gunn[d], J. Holtzman[e], D. Nidever[a], B. Gillespie[f], D. Weinberg[g], B. Blank[h], C. Henderson[h], S. Smee[i], R. Barkhouser[i], A. Harding[i], S. Hope[i], G. Fitzgerald[j], T. Stolberg[j], J. Arns[k], M. Nelson[a], S. Brunner[a], A. Burton[a], E. Walker[a], C. Lam[a], P. Maseman[l], J. Barr[a], F. Leger[m], L. Carey[m], N. MacDonald[m], G. Ebelke[f], S. Beland[n], T. Horne[o], E. Young[p], G. Rieke[l], M. Rieke[l], T. O'Brien[g], J. Crane[q], M. Carr[d], C. Harrison[r], R. Stoll[r], M. Vernieri[r], M. Shetrone[s], C. Allende-Prieto[t], J. Johnson[g], P. Frinchaboy[u], G. Zasowski[a], A. Garcia Perez[a], D. Bizyaev[f], K. Cunha[vwl], V. V. Smith[w], Sz. Meszaros[t], B. Zhao[x] M. Hayden[e], S.D. Chojnowski[a], B. Andrews[g], C. Loomis[d], R. Owen[m], M. Klaene[f], J. Brinkmann[f], F. Stauffer[f], D. Long[f], W. Jordan[f], D. Holder[f], F. Cope[f], T. Naugle[f], B. Pfaffenberger[f], D. Schlegel[y], M. Blanton[z], D. Muna[z], B. Weaver[z], S. Snedden[f], K. Pan[f], H. Brewington[f], E. Malanushenko[f], V. Malanushenko[f], A. Simmons[f], D. Oravetz[f], S. Mahadevan[aa] & S. Halverson[aa]

[a]University of Virginia, 530 McCormick Road, Charlottesville, VA 22904; [b]Gemini Observatory, 670 N. A'ohoku Place, Hilo, HI 96720; [c]Harvard-Smithsonian Center for Astrophysics, 60 Garden Street, MS 20, Cambridge, MA 02138; [d]Princeton University, Peyton Hall, 4 Ivy Lane, Princeton, NJ 08544-1001; [e]Dept of Astronomy, New Mexico State Univ, P. O. Box 30001, MSC 4500, Las Cruces, NM 88003; [f]Apache Point Observatory, 2001 Apache Point Road, P.O. Box 59, Sunspot, NM 88349-0059; [g]The Ohio State University, 140 W. 18th Avenue, Columbus, OH 43210; [h]PulseRay, 4583 State Route 414, Beaver Dams, NY 14812; [i]Johns Hopkins Univ, Dept of Physics & Astronomy, 3400 N Charles St, Baltimore, MD 21218; [j]New England Optical Systems, Inc., 237 Cedar Hill St., Marlborough, MA 01752; [k]Kaiser Optical Systems, Inc., 371 Parkland Plaza, Ann Arbor, MI 48103; [l]Dept of Astronomy/Steward Observatory, Univ of Arizona, 933 N. Cherry Ave, Tucson, AZ 85721; [m]Dept of Astronomy, Box 351580, Univ of Washington, Seattle, WA 98195-1580; [n]APS Department, University of Colorado at Boulder, Boulder, CO 80309; [o]Meinel 733, College of Optical Sciences, Univ of Arizona, 1630 East Univ Blvd, Tucson, AZ 85721; [p]NASA Ames Research Center, Mail Stop 211-3, Moffett Field, CA 94035; [q]Carnegie Observatories, 813 Santa Barbara Street, Pasadena, CA 91101; [r]C Technologies, 757 Route 202/206, Bridgewater, N.J., 08807; [s]McDonald Observatory, Univ of Texas at Austin, HC75 Box 1337-MCD, Fort Davis, TX 79734; [t]Instituto de Astrofísica de Canarias, Vía Lactea S/N, 38205 La Laguna, Tenerife, Spain; [u]Texas Christian University, Box 298840, Fort Worth, TX 76129;[v]Observatorio Nacional, Rio de Janeiro, Brazil; [w]National Optical Astronomy Observatories, PO Box 26732, Tucson, AZ 85726; [x]Dept of Astronomy, Univ of Florida, 211 Bryant Space Science Center, Gainesville, FL 32611; [y]Lawrence Berkeley National Lab, 1 Cyclotron Road MS 50R-5032, Berkeley, CA 94720-8160; [z]Center for Cosmology and Particle Physics, New York University, 4 Washington Place, New York, NY 10003; [aa]Dept of Astronomy & Astrophysics, Penn State University, 525 Davey Lab, University Park, PA, 16802

*jcw6z@virginia.edu; phone 1-434-924-4907; fax 1-434-924-3107

Ground-based and Airborne Instrumentation for Astronomy IV, edited by Ian S. McLean, Suzanne K. Ramsay, Hideki Takami, Proc. of SPIE Vol. 8446, 84460H · © 2012 SPIE · CCC code: 0277-786X/12/$18 · doi: 10.1117/12.927140

Downloaded From: https://www.spiedigitallibrary.org/conference-proceedings-of-spie on 06 Jan 2021
Terms of Use: https://www.spiedigitallibrary.org/terms-of-use

ABSTRACT

The Apache Point Observatory Galactic Evolution Experiment (APOGEE) uses a dedicated 300-fiber, narrow-band near-infrared (1.51-1.7 μm), high resolution (R~22,500) spectrograph to survey approximately 100,000 giant stars across the Milky Way. This three-year survey, in operation since late-summer 2011 as part of the Sloan Digital Sky Survey III (SDSS III), will revolutionize our understanding of the kinematical and chemical enrichment histories of all Galactic stellar populations. We present the performance of the instrument from its first year in operation. The instrument is housed in a separate building adjacent to the 2.5-m SDSS telescope and fed light via approximately 45-meter fiber runs from the telescope. The instrument design includes numerous innovations including a gang connector that allows simultaneous connection of all fibers with a single plug to a telescope cartridge that positions the fibers on the sky, numerous places in the fiber train in which focal ratio degradation had to be minimized, a large mosaic-VPH (290 mm x 475 mm elliptically-shaped recorded area), an f/1.4 six-element refractive camera featuring silicon and fused silica elements with diameters as large as 393 mm, three near-infrared detectors mounted in a 1 x 3 mosaic with sub-pixel translation capability, and all of these components housed within a custom, LN_2-cooled, stainless steel vacuum cryostat with dimensions 1.4-m x 2.3-m x 1.3-m.

Keywords: Spectroscopy, Near-Infrared, Multi-object, Fiber, VPH

1. INTRODUCTION

The Apache Point Observatory Galactic Evolution Experiment (APOGEE) has just completed its first year of a three year survey to observe 100,000 red giant stars in the Milky Way with a dedicated fiber-fed multi-object high-resolution near-infrared spectrograph as part of the Sloan Digital Sky Survey III (SDSS-III).[1] The survey aims to revolutionize our understanding of the chemical and kinematical evolution of all galactic populations. Observing giants in the near-infrared (1.51 – 1.70 μm), where there is much less attenuation from dust compared to optical wavelengths, enables a uniform survey of all galactic populations such as the disk, bulge and halo. And the wavelength range of APOGEE, coupled with a resolution R~22,500, provides access to spectral lines of numerous atomic and molecular species which allows the determination of abundances for 15 chemical elements including Fe, C, N, O, α-elements, odd-Z elements, and some Fe-peak elements.

Following delivery of the instrument in April 2012 and summer-time commissioning, the instrument has been taking survey data since September 2012. So far, 125,000 science spectra have been collected with the instrument to S/N~60. Ultimately, spectra of 100,000 giants will be taken over multiple visits to give S/N~100 which should allow chemical abundance determinations with ~0.1 dex precision.

Section 2 gives an overview of the instrument design and highlights several critical assemblies. Section 3 describes the typical nightly operations, Section 4 presents performance details of the spectrograph and Section 5 highlights some early science results.

2. INSTRUMENT DESIGN

Linked by a ~45-m fiber-feed from the Sloan 2.5-m Telescope at Apache Point Observatory (Sunspot, NM), the APOGEE spectrograph,[2] located in a lab adjacent to the telescope, can observe 300 objects simultaneously. The instrument system includes numerous innovations including a gang connector that allows simultaneous connection of all fibers with a single plug to a telescope cartridge that positions the fibers on the sky, numerous places in the fiber train in which focal ratio degradation (FRD) had to be minimized,[3] a large mosaic volume phase holographic (VPH) grating (290 mm x 475 mm elliptically-shaped recorded area),[4] an f/1.4 six-element refractive camera featuring silicon and fused silica elements with diameters as large as 393 mm, three near-infrared detectors mounted in a 1 x 3 mosaic with sub-pixel translation capability, and all of these components housed within a custom, LN2-cooled, stainless steel vacuum cryostat with dimensions 1.4-m x 2.3-m x 1.3-m.[5]

Downloaded From: https://www.spiedigitallibrary.org/conference-proceedings-of-spie on 06 Jan 2021
Terms of Use: https://www.spiedigitallibrary.org/terms-of-use

2.1 Fiber Assembly

The APOGEE survey leverages the mature plug plate technology of the SDSS system. Eight cartridges are prepared in the day prior to the night's observing. Each cartridge contains a plate pre-drilled with holes for fibers at the location of objects we wish to observe on a particular 3 deg diameter field on the sky. In the case of APOGEE, the holes are drilled to accept stainless steel ferrules which contain Polymicro FIP 120170190 low-OH fibers.

In contrast to the swappable cartridges at the telescope, the fibers at the other end of the train, the pseudo-slit inside the instrument, are permanently installed within the cryogenic environment. Thus a so-called 'gang connector' was developed to enable rapid connection of the 300-fiber umbilical originating within the instrument with successive cartridges throughout the night. Each gang connector allows simultaneous connection of ten custom US Conec (Hickory, NC) 32-fiber connectors in a stress free manner. Each of the ten US Conec connectors contain 30 science fibers.

There are no other fiber-fiber connections in the fiber train so as to minimize FRD. In particular, the fiber penetrates the vacuum vessel without break through custom stainless steel feedthroughs containing 1 cm of Master Bond EP37-3 FLAO epoxy to maintain vacuum integrity while minimizing stress.

Once inside the cryostat, the fiber is routed over a 2-m distance to the pseudo-slit. Each of the ten sets of 30 fibers terminate in a v-groove block assembly. Individual fibers are embedded within grooves with Lord 3170 epoxy and a cap covers each set. A39 is used for the v-grooves and caps as this material has a close match to the coefficient of thermal expansion (CTE) of fused silica. The v-groove assemblies are individually arranged to form a polygon approximation of a curved pseudo slit that not only conforms to the radius of curvature necessary for a Schmidt-style collimator but also curves in a sideways direction. This latter curvature is done so that the slit image at the detector is straightened, thus maximizing use of the detector area. The fiber assemblies were fabricated by C Technologies (Bridgewater, NJ) after FRD testing informed the choice of materials and design.

2.2 Cryostat

A custom stainless steel LN_2-cooled cryostat was designed and fabricated by PulseRay Machining & Design (Beaver Dams, NY). The cryostat waist is fabricated from dual box beams. Top and bottom lids in the shape of half-cylinders attach to the waist and seal with o-rings. Taking advantage of the constant gravity vector inherent in an instrument sited in a lab, the cold plate is suspended from the inside walls of the cryostat by three sets of two stainless steel rods. A 93-liter LN_2 tank is in turn secured to the bottom of the light-weighted cold plate.

A radiation shield system encloses the cold plate, optics (installed on top of the cold plate) and LN_2 tank (below the plate). The system includes two poles, located in the middle of the cold plate, to provide additional thermal connection between the upper radiation shield and the cold plate. While the detector assembly physically attaches to the back of the camera barrel, it is thermally isolated from it through the use of low thermal conductivity materials (e.g. titanium and G-10) in various parts of the detector assembly. Along with this thermal isolation from the rest of the optics, the detector assembly is directly connected to the LN_2 tank through a system of copper braids and a copper pole secured directly to the top of the LN_2 tank through a hole in the cold plate. In contrast, all other optical components are cooled by their physical connections to the top of the cold plate.

Internal heat load is further reduced through an extensive use of blankets of multi-layer insulation. The blankets are custom made to conform to the radiation shield contours and contain ten layers of double-sided aluminized mylar insulation interspersed with toule (bridal veil). In addition, a single sheet of aluminized mylar is taped to the inside wall of the cryostat to reduce emissivity.

2.3 Optical Design

The optical design (Figure 1) is relatively straightforward optically but made difficult in practice because of the large optics. Accumulated FRD from the fiber assembly causes the f/5 telescope beam to speed up to ~f/3.5 upon exit from the fibers at the slit. The light is collimated by Schmidt-style fore-optics in which a spherical mirror with 2106.73 mm nominal radius of curvature is placed at approximately the same distance away from the pupil. The pseudo-slit is placed halfway between the pupil and collimating mirror. The dispersing optic (VPH) is mounted close to the pupil. The collimator is a naturally light-weighted Hextek Corp. (Tucson, AZ) Gas-Fusion^{TM} mirror secured to a mount which provides tip-tilt-piston control while the instrument is cold for focus and alignment adjustment.

Downloaded From: https://www.spiedigitallibrary.org/conference-proceedings-of-spie on 06 Jan 2021
Terms of Use: https://www.spiedigitallibrary.org/terms-of-use

Two fold mirrors, one between the pseudo-slit and collimator, and one between the pseudo-slit and pupil, are used for packaging purposes. The pseudo-slit is on-axis such that the central portion of the collimated beam headed towards the VPH suffers a vertical obscuration from the slit.

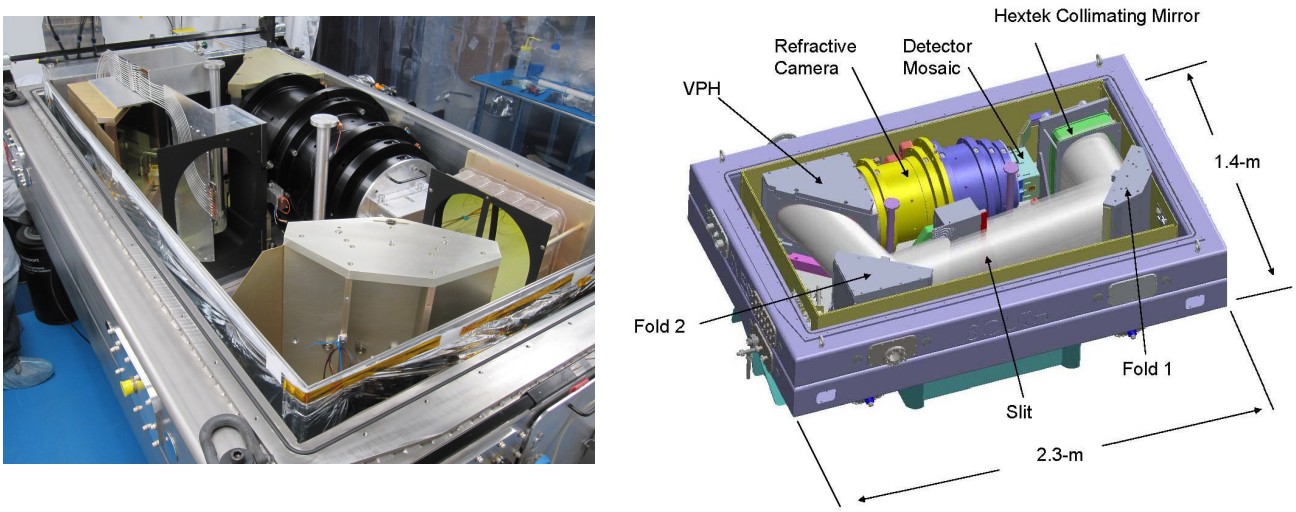

Figure 1. Completed instrument in the lab at Apache Point Observatory (left) and schematic (right).

A VPH fabricated by Kaiser Optical Systems Inc. (Ann Arbor, MI) is used as the dispersing optic. Given the size of the collimated beam (280 mm diameter), only a transmissive grating could be used --- a reflective grating would require an impossibly large (and fast) camera since it would have to be mounted far enough from the grating to allow room for the reflected, and dispersed, beam to clear the incoming beam of the grating. The mosaic VPH was made by making three exposures in gelatin in close succession on a common substrate. The substrate was precisely translated between exposures. The VPH is used in Littrow mode with a 54 deg angle of incidence. This relatively steep angle, along with the size of the collimated beam, required a 290 mm x 475 mm elliptical shaped recorded area.

The dispersed light is brought to a focus on the detectors by a large six-element camera designed, fabricated and tested by New England Optical Systems Inc. (Marlborough, MA). The f/1.4 camera features four mono-crystalline (high-resistivity, slip-free) silicon elements and two Corning 7980 Fused Silica elements. The largest element has a diameter of 393 mm. Overall the camera weighs approx. 250 lb (1110 N). Prior to delivery, camera performance was verified at 1.55 μm with a laser unequal path interferometer and a warm InGaAs camera.

2.4 Detector & Electronics

Three Teledyne Imaging Sensors H2RG 4-output detectors mounted in a 1 x 3 mosaic record the spectra. The detectors are mounted in an assembly similar to the one used for NIRCam on JWST. A sub-pixel translation capability is also provided through the use of a fine pitched screw, rotated by a cyrogenic stepper motor, that drives a traveling lead screw to convert rotation to translation. The traveling lead screw in turn pushes a 12.7:1 lever arm to ultimately provide 0.5 μm displacements for each four steps of a 200-step Phytron cryogenic motor. A rounded nose protruding into the detector assembly applies this displacement to the detector mount. The mount is suspended from flex-pivots that provide compliance in the dithering direction. Copper braids used for thermal connections to the detector mount provide sufficient pre-load to keep the rounded nose in contact with the detector mount.

This mechanism, shown in Figure 2, allows the detectors to dither together in the dispersion direction between integrations by 0.5 pixels. As will be discussed in Section 5.1, the line spread function on the blue end of the APOGEE wavelength range is under-sampled and dithering allows optimal sampling to be recovered. The actual unit performance on the sky meets the specifications of 0.5 ± 0.028 pixel moves.

Downloaded From: https://www.spiedigitallibrary.org/conference-proceedings-of-spie on 06 Jan 2021
Terms of Use: https://www.spiedigitallibrary.org/terms-of-use

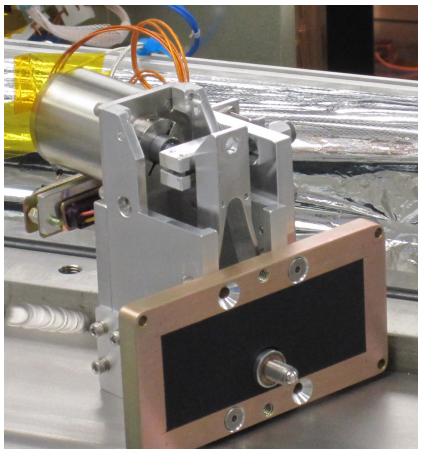

Figure 2. The cryogenic dithering mechanism prior to installation. The rounded nose which displaces the detector mount is in the foreground.

Leach electronics with single video and clock/bias cards are used to operate all 12 outputs (four from each detector) together. A custom cold fanout board is used inside the cryostat to multiplex the cabling from one controller to three detectors. The detectors are run in sample-up-the-ramp (SUTR) mode.

2.5 Calibration Unit

The calibration unit for APOGEE consists of a 6-inch (152.4 mm) integrating sphere from Labsphere (North Sutton, NH). Several light sources can illuminate the sphere through side ports, including two hollow cathode lamps (UNe and ThArNe) which each mount directly to ports. A third port allows fiber-fed light from a Tungsten Halogen flat lamp to illuminate the sphere.

Light from the sphere's exit port illuminates calibration fibers at f/5 to mimic the telescope. For stray light protection the exit port also includes an electronic shutter to keep light off the fibers except during calibration. Either so-called 'dense pack' (all 300 fibers are illuminated) or 'sparse pack' (every sixth fiber is illuminated) can be chosen. This choice is made by connecting the gang connector, previously discussed in Section 2.1, into special receptacles on a podium adjacent to the telescope. These receptacles are connected by fibers to the calibration unit.

3. ASSEMBLY AND ALIGNMENT

3.1 Assembly

Only 18 months separated the instrument Critical Design Review and delivery of the instrument to the telescope. This fast paced development schedule necessitated a design and fabrication concept in which we distributed the development of sub-modules to collaborating institutions and vendors in a closely-knit teaming approach. Delivered modules were integrated and aligned within the cryostat at the University of Virginia prior to end-end system testing.

3.2 Alignment

The fore-optics were aligned using a He-Ne laser iteratively aligned with pin-holes temporarily installed along the optical path. In this way the the path composed of Fold 1 – Collimator – Fold 1 – Fold 2 – VPH was aligned. Both pads, which set the location of optics within their mounts, and 'bumpers', which set the position of the mounts themselves relative to the cold plate, were adjusted (re-machined) as required. The He-Ne laser could not be used to check the camera position as the silicon elements in the camera are opaque to visible light. The camera was simply placed at the design location and verified as well as possible with machine shop measuring tools.

Once all of the optics were positioned, overall imaging performance was tested warm with an InGaAs camera in the instrument focal plane. A proxy for the pseudo-slit was used which allowed the placement of a fiber source at either the

Downloaded From: https://www.spiedigitallibrary.org/conference-proceedings-of-spie on 06 Jan 2021
Terms of Use: https://www.spiedigitallibrary.org/terms-of-use

first, middle, or last fiber of the set of 300, thus allowing a check of on-axis and off-axis performance. Warm imaging was done before and after the first system cooldown to ensure all optics, particularly the VPH and camera, successfully withstood the cryogenic cycle. The warm imaging included use of a Hartmann mask at the entrance of the VPH in which subsets of mask holes covered the different recorded panels of the VPH. Given the degraded imaging performance of the instrument while warm (it was optimized for cold use), and the large pixels of the InGaAs camera (40 μm), our ability to make detailed image performance checks while warm was limited. Nonetheless, to the extent possible, no evidence was seen that light transmitted through the different VPH panels came to a focus at different locations in the focal plane.

Following warm testing, the instrument was iteratively cold tested with the actual focal plane assembly and a successively larger complement of sets of v-groove blocks until all 300 fibers had been installed. Through these cold tests the detector read-out scheme was fine-tuned and noise performance was evaluated and optimized. Also, the collimator was translated in piston in real-time while cold to produce focus curves, evaluate imaging performance, and find the best focus position for the detector package relative to the end of the camera barrel.

During lab testing we discovered the instrument suffered from a large amount of astigmatism. While we do not know the ultimate source of the astigmatism, it is manifested by the spectral direction coming to a focus sooner (closer to the end of the camera) than the spatial direction. Because it was seen at all field angles, including on-axis, the astigmatism is not thought to be in the camera. This suspicion is corroborated by the fact that spectral and spatial alignment was excellent – all expected wavelengths and all 300 fibers were imaged on the focal planes as designed.

The astigmatism is more likely due to some optic in collimated light, i.e. the collimator, a fold mirror, or the VPH. (We know it is not in the Fold 1 – Collimator – Fold 1 segment when warm: These optics were tested warm with a laser unequal path interferometer and did not have astigmatism.) Not knowing the actual source of the aberration, we successfully mimicked the focus curves observed in the lab by adding ~20 waves (at 0.6328 nm) of astigmatism to the collimator in the Zemax™ instrument optical design. Physically this aberration corresponds to the top and bottom edges of the collimator being pulled back by ~13 μm.

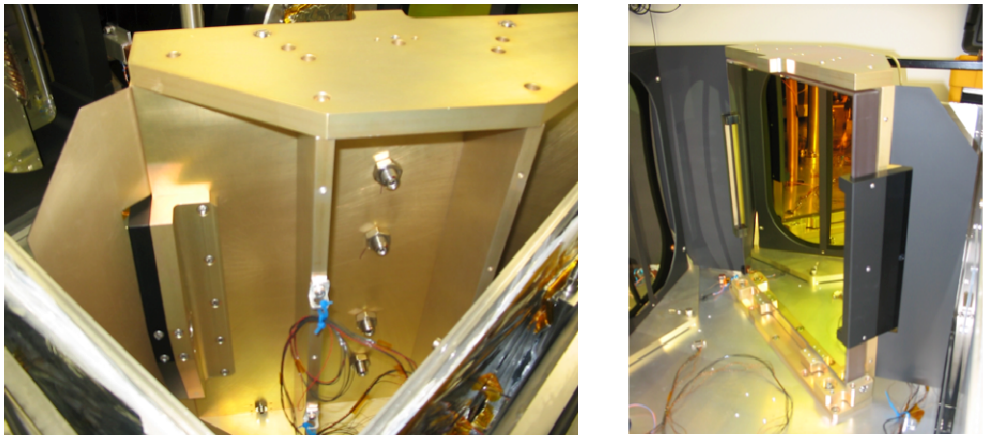

Figure 3. Fold 1 mount with modifications to bend the mirror along its vertical mid-line. (Left) The four spring plungers pushing on the back of the mirror. On the left side of the image is whiffle tree which allows two hard points on the front of the mirror to act as one. (Right) View of the front of the mirror with its hard points.

We largely eliminated the astigmatism by bending Fold 1 into a cylindrical shape to reduce power in the spectral direction. As Fold 1 is used in double-pass, the effect of its bending is applied twice. Figure 3 shows the mirror in its bent configuration. Approx. 3 μm sag is induced in the mirror by exerting ~ 160 lbf (711 N) distributed across four spring plungers along the back vertical spine of the mirror. Such a large force is necessary as the mirror is 1.5 in (39.1 mm) thick. The mirror mount includes three hard points on the front, one of which is actually a wiffle tree that transfers two hard points to one along one of the sides.

Downloaded From: https://www.spiedigitallibrary.org/conference-proceedings-of-spie on 06 Jan 2021
Terms of Use: https://www.spiedigitallibrary.org/terms-of-use

3.3 Detector Fine-Tuning

Individual detector positions are set by precision lapped shims between the sensor chip assemblies and a mounting plate which holds all detectors. Globally, the position of all three detectors as a unit can be adjusted relative to the back of the camera with a set of three hand-lapped shims. In practice, the middle detector orientation is set with the global shims on the back of the camera. The relative orientation of the blue and red detectors is adjusted individually with respect to the middle detector. Adjustment of global shims is straightforward. On the other hand, adjustment of individual detector shims requires disassembly of the detector package and direct handling of the detector.

To mitigate the chance of damage to the detectors, individual shim adjustments were only done at the University of Arizona where the detector assembly was fabricated and assembled. During the summer commissioning the detector package was removed from the instrument and transported to the University of Arizona for adjustment of the red detector relative position as it was originally out of focus and tilted relative to its ideal position.

4. OPERATIONS

4.1 Observing Cadence

Most survey fields are observed on at least three different nights (epochs) to build up S/N and allow a check for binarity. On a given night, the fields are observed for approx. 1 hour total integration time. Specifically, 8 frames composed of the detector dither positions ABBAABBA are exposed where each frame is made up of 47 sample-up-the-ramp reads and each read is approx. 10 seconds.

4.2 Calibration Sequences

Calibration sequences are taken during the afternoon before the start of observing, interspersed between nighttime fields, and in the morning after observations. Evening and morning calibration sequences include long darks, a flat field with the quartz tungsten halogen lamp, ThArNe and UNe hollow cathode lamp integrations at each dither position, and internal flat fields (using infrared LED's mounted to the cold shutter). Dome flat fields are taken after each field is observed during the night.

4.3 Spectral Reduction and Abundance Pipelines

Spectra are typically extracted within a couple of days of observation by a robust, automated extraction pipeline. While under continuing development, it handles all facets of data reduction including production of 1-d calibrated spectra, estimation of stellar physical parameters (metallicity [Fe/H], effective temperature T_{eff}, and gravity log(g)) and radial velocity determination.

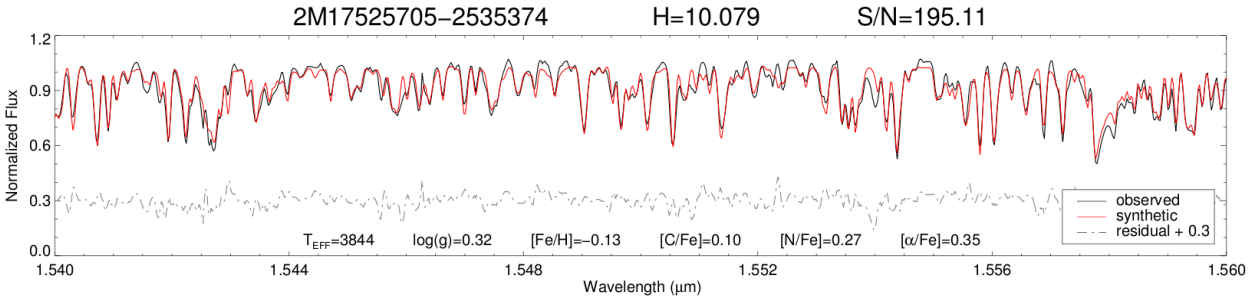

Figure 4. A segment of a reduced spectrum for a bulge star with metallicity [Fe/H] ~ -0.1. The reduced spectrum and preliminary ASPCAP synthetic spectrum are shown along with residuals.

The APOGEE Stellar Parameters and Chemical Abundances Pipeline (ASPCAP) is also being developed to determine stellar parameters and abundances of the various elements measurable from the APOGEE spectra. This pipeline is extremely ambitious – while to date most astronomical high-resolution spectra have been reduced by hand, an automated process must be used for APOGEE given our goal of surveying 100,000 stars. Figure 4 shows an example extraction overplotted with a best fit synthesized spectrum from ASPCAP.

Downloaded From: https://www.spiedigitallibrary.org/conference-proceedings-of-spie on 06 Jan 2021
Terms of Use: https://www.spiedigitallibrary.org/terms-of-use

5. SPECTROGRAPH PERFORMANCE

5.1 Resolution & Sampling

The instrument meets its science requirement of R~22,500 as seen in Figure 5. Shown are measurements of line spread function FWHM and implied resolution for a variety of UNe hollow cathode lamp wavelengths across all three detectors at the top, middle and bottom field angles. Outliers are thought to be due to a variety of causes such as imperfect positioning of individual v-groove blocks relative to optimal focus, non-uniform flatness of the arrays, and spectral lines which are close-blends and thus masquerade as lines with larger line spread functions.

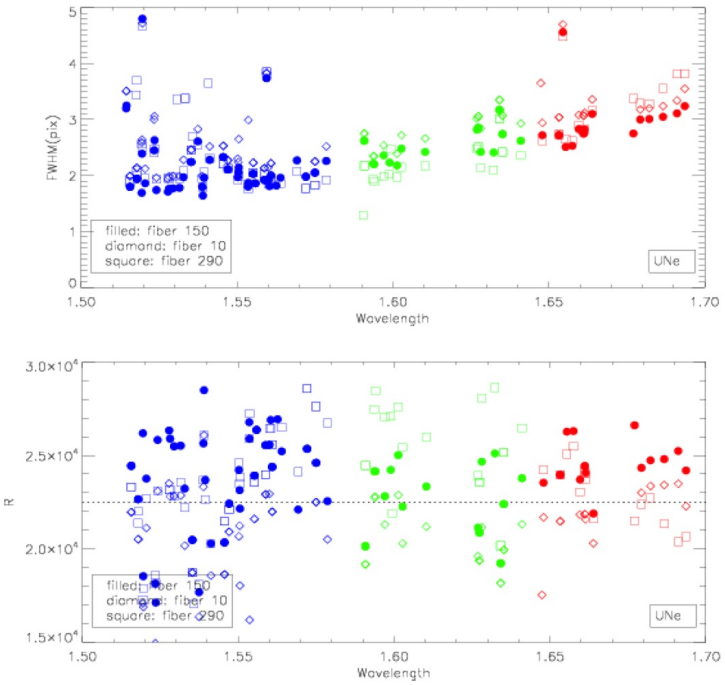

Figure 5. Measured line spread function FWHM and implied resolution from calibration UNe hollow cathode lamp lines.

5.2 Throughput

Science requirements for throughput were the ability to achieve S/N = 100 per pixel for *H* =12.2 stars with a 3-hour integration. Analysis of frames observed through December 2012 show that we should meet this requirement for the blue and middle chips but fall short for the red chip. A tally of as-built component efficiencies suggested total instrument throughput of ~33%, 43% and 23% for the blue, middle and red detectors, respectively, including the fiber entrance at the telescope through the detectors, but not including losses from the atmosphere, telescope, or effects of seeing on light spread at the fiber entrance. The fall-off in the red throughput is largely due to the VPH grating efficiency which falls to ~45% at the red edge of the wavelength coverage. This red fall-off was accepted at the time of instrument design. Lastly, on-telescope performance suggests 16 % broad-band *H* throughput including the atmosphere, telescope, fiber system and instrument.

5.3 Cryostat Performance

The APOGEE cryostat performance has been very reliable. The LN_2 tank consumes 17 liters/day to offset the ~30 W heat load. Given its 93 liter tank, the instrument has a comfortable hold time of 5.5 days while operating. LN_2 is topped-off each morning following calibration exposures by an automated fill system from American Magnetics (Oak

Downloaded From: https://www.spiedigitallibrary.org/conference-proceedings-of-spie on 06 Jan 2021
Terms of Use: https://www.spiedigitallibrary.org/terms-of-use

Ridge, TN). In addition to providing real-time APOGEE LN_2 tank levels with an embedded capacitive liquid level sensor, the system controls the daily fills based on level thresholds and an external timer.

Figure 6 shows recorded temperatures for the camera and detector along with the atmospheric pressure on the mountain. The top plot shows that the detector temperature closely follows the changes in pressure. This is understandable given the detector assembly has tight thermal coupling to the tank and the LN_2 boil-off temperature changes as a function of atmospheric pressure. In contrast, the 250 lb camera bolted to the cold plate has significant thermal inertia and it has a much longer response time to pressure changes.

While resistive heaters are installed on the detector base plate and a thermal control system is in place, no active detector temperature control has been used thus far in the survey.

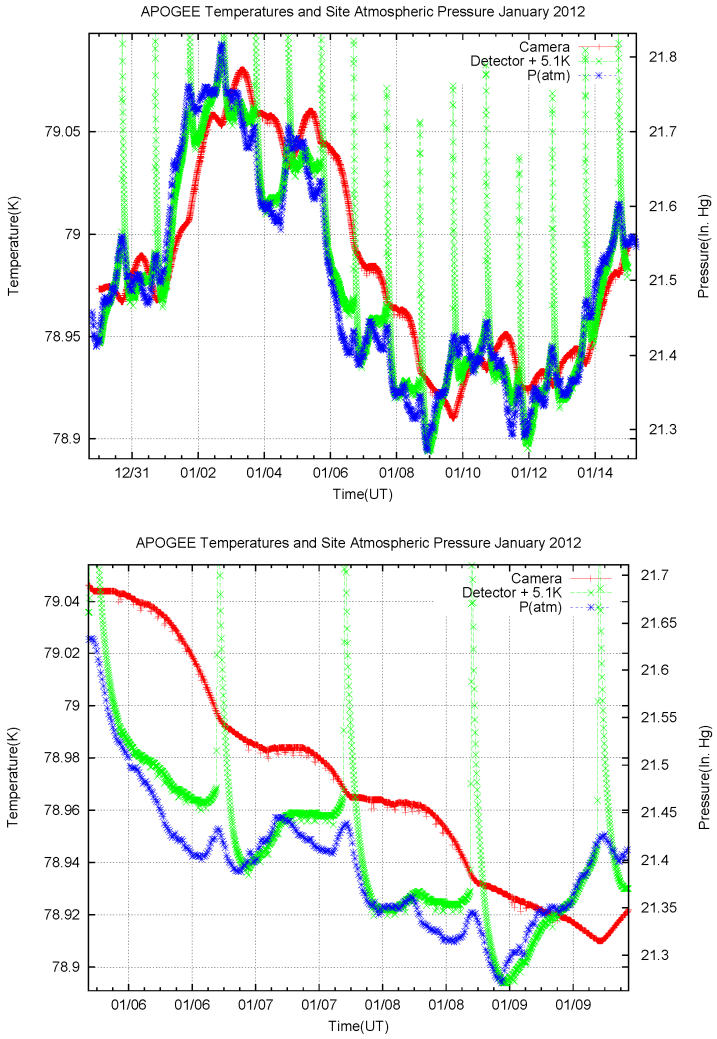

Figure 6. Camera and detector temperatures and mountain atmospheric pressures throughout January 2012 (top) and a three-day portion of that month (bottom).

5.4 Instrument Stability and Radial Velocity Performance

While the cryostat itself has functioned well, the instrument does suffer from unanticipated flexure due to changing gravity load underneath the cold plate as the LN_2 boils-off. We suspect the cold plate was light-weighted too

Downloaded From: https://www.spiedigitallibrary.org/conference-proceedings-of-spie on 06 Jan 2021
Terms of Use: https://www.spiedigitallibrary.org/terms-of-use

aggressively. Nonetheless, the flexure, manifested by a 0.2 pixel shift in the spatial direction of the spectral traces through a 24-hr period, is very repeatable and can be corrected during spectral extraction. In the spectral direction the traces move approx 1/10 as much but in a more complex manner.

Despite this flexure, radial velocity precision has been surprisingly good. While the science requirement was 0.3 km/sec for spectra with S/N = 100 and ~0.5 km/sec for S/N = 60, the instrument and data reduction pipeline is delivering radial velocity precision of ≤ 100 m/sec. Figure 7 shows the radial velocity scatter for all objects with three or more observations and S/N > 20. The long tail of higher radial velocity scatter is thought to be real variations from objects that are in fact binaries.

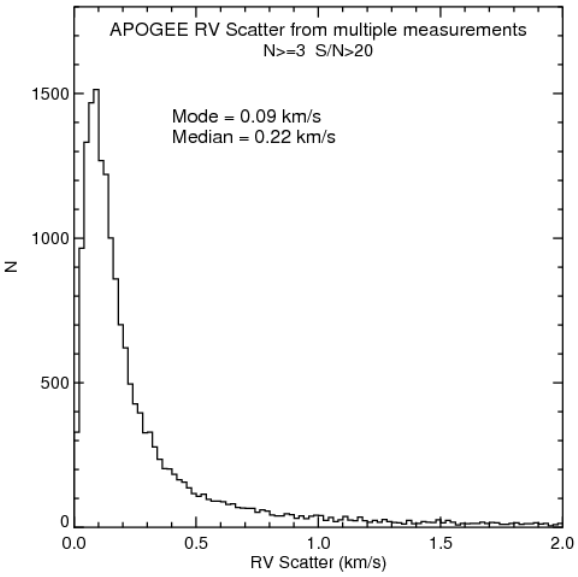

Figure 7. Histogram of radial velocity scatter for objects with three or more observations and S/N > 20. The long tail is thought to reflect real radial velocity variations of binaries.

5.5 VPH performance

Both the VPH Littrow ghost and scattered light intensity have been estimated. The Littrow ghost can occur in all grating spectrographs but is most apparent in instruments that use VPH gratings since they are often used in Littrow mode (angle of incidence = angle of exit), as is the case for APOGEE. The ghost arises from light that reflects off the face of the detector, is transmitted backwards through the camera, and then recombines into a reflected white light spectrum in two different ways within the VPH. This white light spectrum is transmitted back towards the detector a second time and is positioned at the location of the Littrow wavelength.[6] For APOGEE the Littrow wavelength based on as-built optics was predicted to be 1.6028 μm assuming 54 deg angle of incidence. The Littrow ghost is actually located at 1.6048 μm. In APOGEE the ghost appears as a curved spectrum since it is a ghost of the straight spectral images originally falling on the detector.

The Littrow ghost intensity was measured during tests of the Penn State Fiber Fabry Perot (FFP)[7] with APOGEE in February 2012. The FFP is a novel device composed of a single mode fiber with two dielectric stack mirrors spliced into the fibers to form a Fabry Perot cavity. Contained within a ~5 cm x 1 cm x 1 cm casing, the device also includes a thermistor and thermo-electric cooler for precise temperature control. Illuminated by a super-continuum laser source, approx. 400 discrete spectral lines are recorded for each fiber on the three APOGEE detectors. Thus 120,000 lines are recorded on the three chips when all 300 fibers are included. APOGEE observed the FFP illumination via the calibration

Downloaded From: https://www.spiedigitallibrary.org/conference-proceedings-of-spie on 06 Jan 2021
Terms of Use: https://www.spiedigitallibrary.org/terms-of-use

system integrating sphere. Figure 8 shows the co-added image representing a 39,000 second integration from a sequence of overnight frames.

Analysis of the raw image gives a ghost intensity of ~0.004 relative to the total intensity of light originally falling on the detectors. While this Littrow ghost strength conforms to predictions by Burgh et al.,[6] it is nearly a factor of four stronger than our predictions based on the individual efficiencies of the various optical components that contribute to overall ghost strength. A proper estimate of Littrow ghost strength would require detailed testing of VPH efficiencies for orders other than zero and the first order transmission. These efficiencies are on average less than 1% and vary by wavelength which make such measurements difficult. Also, detailed knowledge of the camera vignetting as a function of wavelength and field are necessary for the calculation. In the event, this is mainly academic for APOGEE – the Littrow ghost falls in an area on the middle chip which is largely devoid of important spectral lines necessary for abundance analysis.

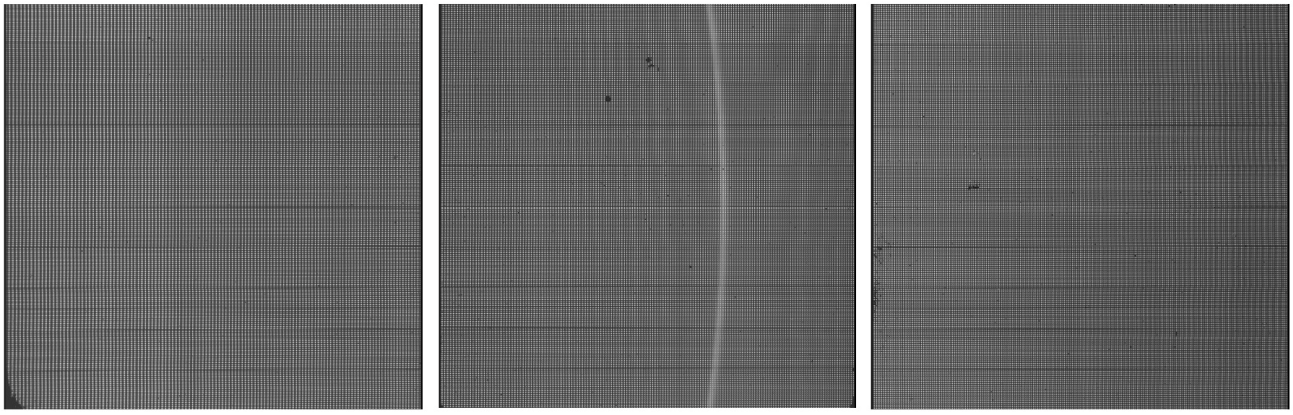

Figure 8. The Littrow ghost (right side of the middle chip) seen in a co-added spectrum with a total integration time of 39,000 seconds. From left to right the detectors are red, middle and blue.

Imperfections in grating ruling periodicities and cosmetic features cause scattered light far beyond the central line. In fact this scattered light is believed to be the cause of what is interpreted to be OH-continuum between the bright OH lines in the near-infrared.[8] Scattered light from the APOGEE VPH was also tested during February 2012 using a 1550.60 nm laser which illuminated the integrating sphere in a similar manner as the FFP. The wings of the line spread function of the co-added image from overnight frames was fit with the following equation developed by Woods et al. 1994 to describe the scattered-light profile:

$$Y_{fit} = \left[\frac{\mathrm{sinc}(b)}{\mathrm{sinc}(b_o)}\right]^2 \frac{0.5}{N^2 \sin^2 a} + A_B$$

In this equation N is interpreted to be the "approx. smallest number of consecutive grooves with no imperfections" and A_B is an additive background.[9]

Downloaded From: https://www.spiedigitallibrary.org/conference-proceedings-of-spie on 06 Jan 2021
Terms of Use: https://www.spiedigitallibrary.org/terms-of-use

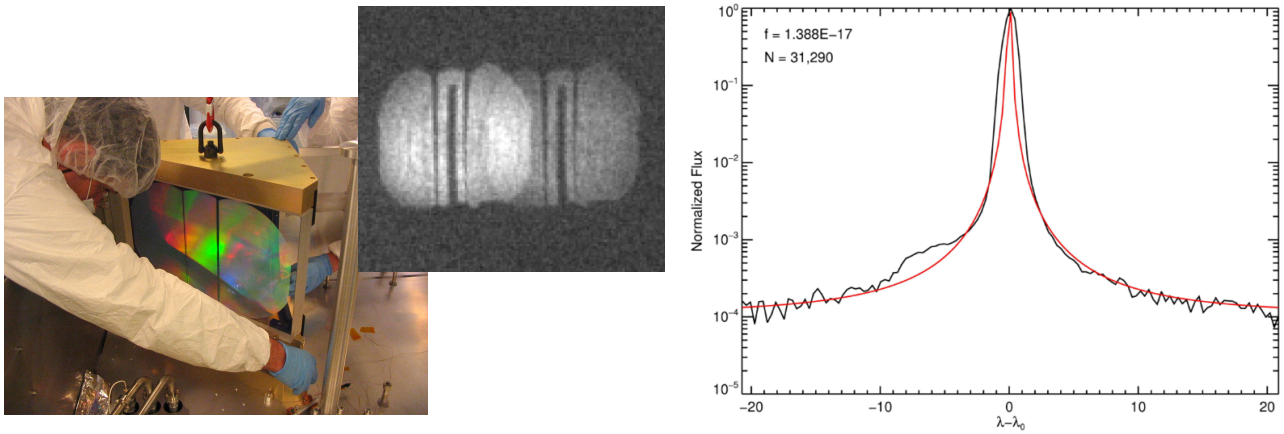

Figure 9. (Left and middle) A picture of the VPH as it was installed and warm pupil images of two spectral lines. (Right) The scattered light profile of the 1.5506 μm laser line dispersed by the APOGEE VPH. The x-axis coordinates are Angstroms. Since APOGEE pixels are ~0.3 Angstroms, the x-axis spans ± 66 pixels.

The fit to the wings of the APOGEE line spread function, shown in Figure 9, gives $N \sim 30{,}000$. This is in fact the smallest number of consecutive grooves geometrically illuminated within the instrument. Warm pupil images, recorded by observing two spectral lines within APOGEE far out of focus with an InGaAs camera, are shown in Figure 9, along with a picture of the VPH being installed into the instrument. The shadow of the pseudo-slit central obscuration can be seen against the small inner rectangular recorded panel. The illuminated portion of that rectangle, to the left and right of the shadow, in fact contain approx. 30,000 recorded lines. This cannot be interpreted to mean the *entire* VPH is pristine as the larger side panels could in fact contain consecutive segments without imperfections that contain more than 30,000 lines. Nonetheless, this does suggest the VPH recording is very good.

5.6 High-persistence

A portion of the blue detector contains abnormal persistence compared to the rest of the detector. Confined to an area in the top one-third of the detector, this abnormal persistence is nearly 20 times stronger than elsewhere on the detector. Figure 10 includes an image seven minutes after a flat field. The figure also shows the integrated persistence of the abnormally high and normal persistence regions of the array as a function of time after illumination to approx. 40,000 counts.

Because of this abnormal persistence, we installed a cold shutter inside the instrument during commissioning. When closed, the shutter covers the pseudo-slit with a light-tight enclosure to prevent inadvertent illumination of the detectors. In addition, observing procedures and automated observing routines have been established to minimize all unnecessary light from falling on the arrays, particularly during cartridge changes.

Since we have not found a way to reduce the persistence, we are attempting to correct for the persistence during spectral extraction by using forward modeling techniques in which prior illumination is tracked and the resultant persistence is estimated and subtracted.

Downloaded From: https://www.spiedigitallibrary.org/conference-proceedings-of-spie on 06 Jan 2021
Terms of Use: https://www.spiedigitallibrary.org/terms-of-use

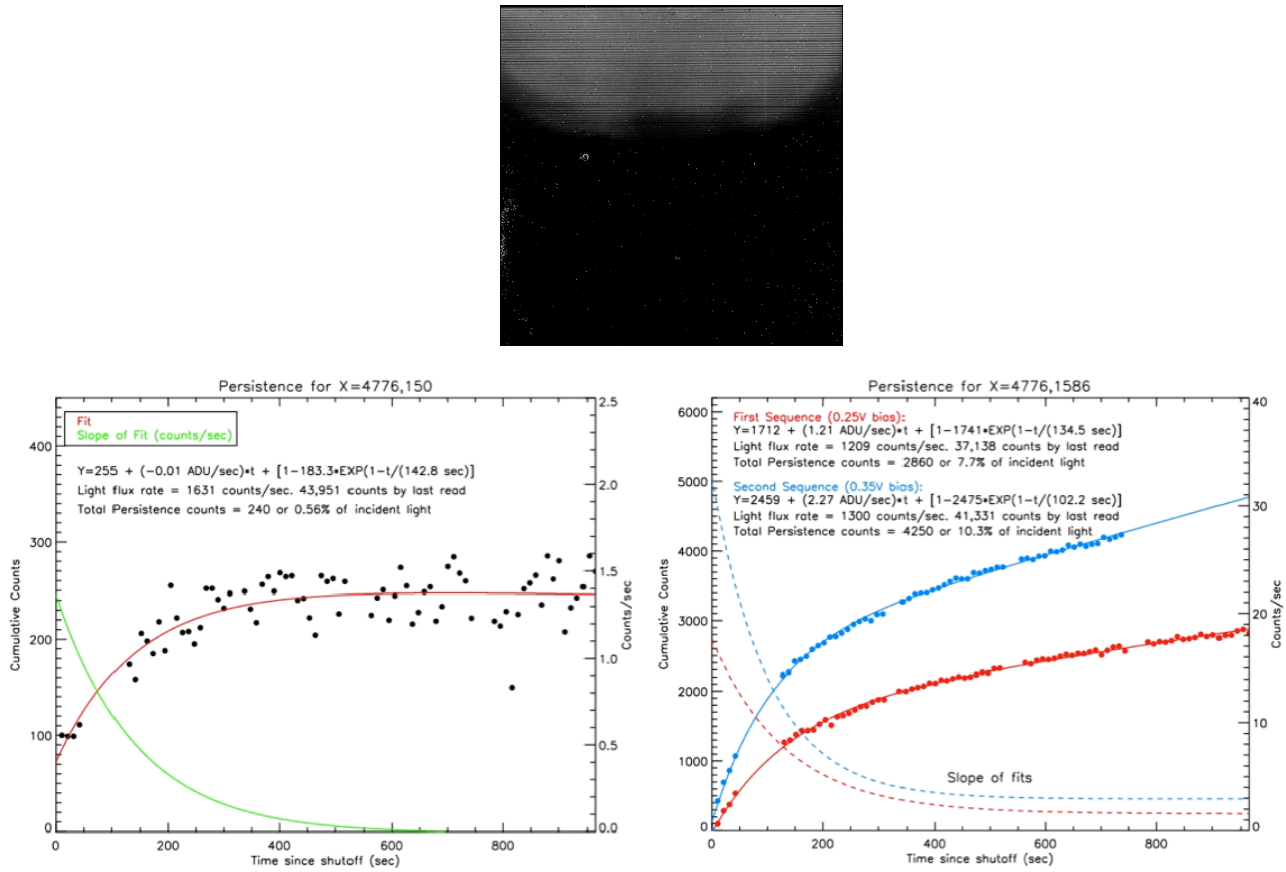

Figure 10. (Left) The blue detector 7 minutes after flat-field illumination. Abnormally high persistence is seen in the top 1/3 of the detector. (Right) Plots of persistence v. time for the abnormally high (top) and normal (bottom) persistence regions.

6. EARLY SCIENCE RESULTS

6.1 Bulge Kinematics

Observations of K and M-giants in the Galactic bulge taken last summer during commissioning have revealed a new kinematic population of stars thought to be in orbits around the Galactic bar potential.[10] The sample of 4,700 stars observed in the bulge is the largest set of high resolution, near-infrared spectra ever taken. While most of the stars had radial velocities distributed around the Galactic standard of rest (V_{GSR} ~ 0 km/sec), about 10% of the stars in the sample had radial velocities of V_{GSR} ~ +200 km/sec with relatively low (cold) velocity dispersion of σ_V ~ 30 km/sec. This new population doesn't conform to simple models of stars on circular orbits about the Galactic center. Comparison to various Galactic models suggests that these high radial velocities are best explained by stars in orbits of the Galactic bar potential, although some observational features remain unexplained.

6.2 Recovery of a Known Extra-solar Planet

As we mentioned in Section 4.1, most stars in the APOGEE sample are observed three different times to check for changing radial velocity and hence binarity. But a subset of the APOGEE sample are observed up to 24 times, usually to build up signal to noise for fainter objects. Analysis of ~1300 stars with at least 8 APOGEE visits flagged about 130 objects as potentially harboring planet/brown dwarf candidates. It turned out that one of the objects was HD 114762, an object already known to have an orbiting low-mass companion thought to be an extrasolar planet.[11,12] Thus APOGEE inadvertently (re-)discovered its first likely extrasolar planet, HD 114762b. Figure 11 shows good agreement between

Downloaded From: https://www.spiedigitallibrary.org/conference-proceedings-of-spie on 06 Jan 2021
Terms of Use: https://www.spiedigitallibrary.org/terms-of-use

the published orbital parameters for the system along with those calculated with automated and hand-fitting of the APOGEE data. Also shown is a phase-folded orbital fit using a two-dimensional correlation technique known as TODCOR[13] on the APOGEE data. The fit yields an RMS of 33 m/sec. Interestingly, several of the RV data points were taken prior to opening the cryostat for summertime optics adjustments. Recovery of this likely extrasolar planet is good evidence of the APOGEE instrument stability and is a harbinger of its potential for finding new low-mass companions.

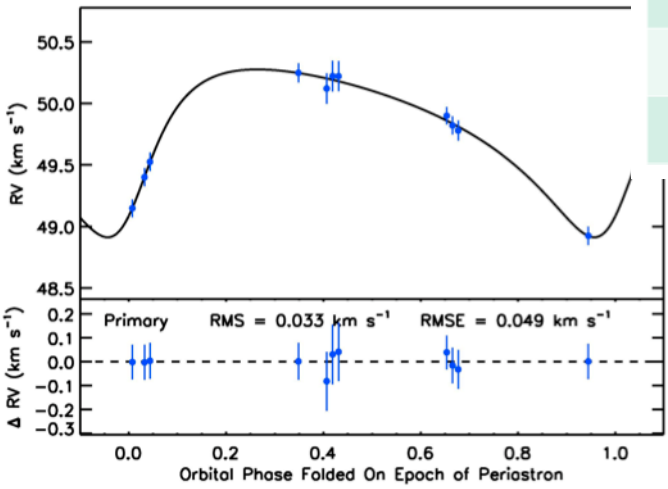

source	K (m/s)	P (days)	e	Ω (deg)	$M_2 sini$ (M_{jup})
published	616	83.9	0.34	202	11
automated fitting APOGEE data	590	77.9	0.01	176	14
hand fitting of APOGEE data	682	81.7	0.44	221.8	

Figure 11. (Top right) Comparison of the published orbital parameters for the HD 114762 system and those determined by automated and hand fitting with APOGEE data. (Bottom left) A phase folded orbital solution using TODCOR and the APOGEE data.

ACKNOWLEDGEMENTS

Funding for SDSS-III has been provided by the Alfred P. Sloan Foundation, the Participating Institutions, the National Science Foundation, and the U.S. Department of Energy Office of Science. The SDSS-III web site is http://www.sdss3.org/. SDSS-III is managed by the Astrophysical Research Consortium for the Participating Institutions of the SDSS-III Collaboration including the University of Arizona, the Brazilian Participation Group, Brookhaven National Laboratory, University of Cambridge, Carnegie Mellon University, University of Florida, the French Participation Group, the German Participation Group, Harvard University, the Instituto de Astrofisica de Canarias, the Michigan State/Notre Dame/JINA Participation Group, Johns Hopkins University, Lawrence Berkeley National Laboratory, Max Planck Institute for Astrophysics, Max Planck Institute for Extraterrestrial Physics, New Mexico State University, New York University, Ohio State University, Pennsylvania State University, University of Portsmouth, Princeton University, the Spanish Participation Group, University of Tokyo, University of Utah, Vanderbilt University, University of Virginia, University of Washington, and Yale University.

REFERENCES

[1] Eisenstein, D. J. et. al., "SDSS-III: Massive Spectroscopic Surveys of the Distant Universe, the Milky Way, and Extra-Solar Planetary Systems," AJ, 142, 72 (2011).

[2] Wilson, J. C. et al., "The Apache Point Observatory Galactic Evolution Experiment (APOGEE) high-resolution near-infrared multi-object fiber spectrograph," Proc. SPIE 7735, 77351C (2010).

Downloaded From: https://www.spiedigitallibrary.org/conference-proceedings-of-spie on 06 Jan 2021
Terms of Use: https://www.spiedigitallibrary.org/terms-of-use

[3] Brunner, S., Burton, A., Crane, J., Zhao, B., Hearty, F. R., Wilson, J. C., Carey, L., Leger, F., Skrutskie, M., Schiavon, R. and Majewski, S. R., "APOGEE fiber development and FRD testing," Proc. SPIE 7735, 77356A (2010).
[4] Arns, J., Wilson, J. C., Skrutskie, M., Smee, S., Barkhouser, R., Eisenstein, D., Gunn, J., Hearty, F., Harding, A., Maseman, P., Holtzman, J., Schiavon, R., Gillespie, B. and Majewski, S., "Development of a large mosaic volume phase holographic (VPH) grating for APOGEE," Proc. SPIE 7739, 773913 (2010).
[5] Blank, B., Henderson, C., Wilson, J. C., Hearty, F. R., Skrutskie, M., O'Brien, T. P., Majewski, S. R., Schiavon, R., Maseman, P., Brunner, S., Burton, A. and Walker, E., "APOGEE cryostat design," Proc. SPIE 7735, 773569 (2010).
[6] Burgh, E. B., Bershady, M. A., Westfall, K. B., & Nordsieck, K. H., "Recombination Ghosts in Littrow Configuration: Implications for Spectrographs Using Volume Phase Holographic Gratings," PASP, 119, 1069 (2007).
[7] Halverson, S. Mahadevan, S., Ramsey, L., Redman, S., Nave, G., Wilson, J. C., Hearty, F. and Holtzman, J., "Development of a New, Precise Near-Infrared Doppler Wavelength Reference: A Fiber Fabry-Perot Interferometer," these proceedings.
[8] Ellis, S. C. and Bland-Hawthorn, J., "The case for OH suppression at near-infrared wavelengths," MNRAS, 386, 47 (2008).
[9] Woods, T. N, Wrigley III, R. T., Rottman, G. J. and Haring, R. E., "Scattered-light properties of diffraction gratings," Applied Optics, 33, 4273 (1994).
[10] Nidever, D. L., et al., "The Apache Point Observatory Galactic Evolution Experiment: First Detection of High Velocity Milky Way Bar Stars," ApJL, accepted.
[11] Latham, D. W., Stefanik, R. P., Mazeh, T., Mayor, M. and Burki, G., "The unseen companion of HD114762 - A probable brown dwarf," Nature, 339, 38 (1989).
[12] Marcy, G. W., Butler, R. P., Vogt, S. S., Fischer, D. and Liu, M. C., "Two New Candidate Planets in Eccentric Orbits," ApJ, 520, 239 (1999).
[13] Mazeh, T. and Zucker, S., "TODCOR: A two-dimensional correlation technique to analyze stellar spectra in search of faint companions," Ap&SS, 212, 349 (1994).

Downloaded From: https://www.spiedigitallibrary.org/conference-proceedings-of-spie on 06 Jan 2021
Terms of Use: https://www.spiedigitallibrary.org/terms-of-use